

Vibrio harveyi Flavin Reductase–Luciferase Fusion Protein Mimics a Single-Component Bifunctional Monooxygenase[†]

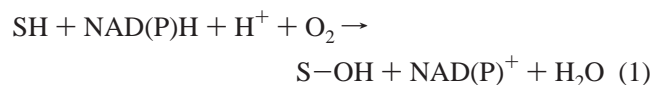
Navneet Jawanda, Kamran Ahmed, and Shiao-Chun Tu*

Department of Biology and Biochemistry, University of Houston, Houston, Texas 77204-5001

Received July 16, 2007; Revised Manuscript Received October 22, 2007

ABSTRACT: *Vibrio harveyi* luciferase and flavin reductase FRP are, together, a two-component monooxygenase couple. The reduced flavin mononucleotide (FMNH₂) generated by FRP must be supplied, through either free diffusion or direct transfer, to luciferase as a substrate. In contrast, single-component bifunctional monooxygenases each contains a bound flavin cofactor and does not require any flavin addition to facilitate catalysis. In this study, we generated and characterized a novel fusion enzyme, FRP- $\alpha\beta$, in which FRP was fused to the luciferase α subunit. Both FRP and luciferase within FRP- $\alpha\beta$ were catalytically active. Kinetic properties characteristic of a direct transfer of FMNH₂ cofactor from FRP to luciferase in a FRP:luciferase noncovalent complex were retained by FRP- $\alpha\beta$. At submicromolar levels, FRP- $\alpha\beta$ was significantly more active than an equal molar mixture of FRP and luciferase in coupled bioluminescence without FMN addition. Importantly, FRP- $\alpha\beta$ gave a higher total quantum output without than with exogenously added FMN. Moreover, effects of increasing concentrations of oxygen on light intensity were investigated using sub-micromolar enzymes, and results indicated that the bioluminescence produced by FRP- $\alpha\beta$ without added flavin was derived from direct transfer of reduced flavin whereas bioluminescence from a mixture of FRP and luciferase with or without exogenously added flavin relied on free-diffusing reduced flavin. Therefore, the overall catalytic reaction of FRP- $\alpha\beta$ without any FMN addition closely mimics that of a single-component bifunctional monooxygenase. This fusion enzyme approach could be useful to other two-component monooxygenases in enhancing the enzyme efficiencies under conditions hindering reduced flavin delivery. Other potential utilities of this approach are discussed.

Many known flavin-dependent monooxygenases belong to the single-component bifunctional group. These enzymes are genuine flavoenzymes, typified by having a tightly bound flavin cofactor, capable of catalyzing the following reaction where SH is a substrate and S–OH is the hydroxylated product (eq 1):



They are “single-component” and “bifunctional” because a single monooxygenase species is capable of catalyzing the reductive (i.e., reducing the flavin cofactor by NADH or NADPH) and the oxidative (i.e., substrate hydroxylation) half reactions. Mammalian flavo-monooxygenases (1) and bacterial *p*-hydroxybenzoate hydroxylase (2), salicylate hydroxylase (3), and 3-hydroxybenzoate-6-hydroxylase (4) are just a few examples of such enzymes.

Lesser known are the “two-component” flavin-dependent monooxygenases, each of which is an enzyme couple consisting of a flavin reductase and a separate “monofunctional” monooxygenase. The latter does not have any flavin cofactor, is inactive in reducing flavin by NAD(P)H, and requires reduced flavin (FH₂) as a substrate for its oxidative

(substrate hydroxylation) activity (eq 2). The required FH₂ can be provided by the flavin reductase component.



For more than three decades, flavin reductase:luciferase couples from luminous bacteria are the only well characterized flavin-dependent two-component monooxygenase system. However, in the past decade or so a rapidly growing number of two-component monooxygenase couples have been identified and characterized (5, 6). The functions of these two-component monooxygenases are quite diverse, ranging from bacterial bioluminescence (7) to desulfurization of fossil fuels (8, 9), biosynthesis of antibiotics (10–14), and hydroxylation of a variety of naturally occurring and man-made substrates (15–31).

A major mechanistic difference between the one-component bifunctional monooxygenases and the two-component monooxygenases is that the former are able to retain the reduced flavin cofactor, once generated, at the active site ready for subsequent catalytic reaction steps whereas the monooxygenase component of the latter group must, one way or another, acquire the reduced flavin provided by the reductase component. Our laboratory has undertaken a series of studies to elucidate the mechanisms of reduced flavin transfer using reductases and luciferases from luminous bacterium strains *Vibrio harveyi* and *Vibrio fischeri*. The NADPH-specific flavin reductase FRP¹ from *V. harveyi* (32)

[†] Supported by grant E-1030 from the Robert A. Welch Foundation.

* Author to whom correspondence should be addressed. E-mail: dtu@uh.edu. Phone: 713-743-8359. Fax: 713-743-8351.

and the NADH-NADPH-utilizing flavin reductase FRG from *V. fischeri* (33) each has a bound FMN cofactor per monomer. We found that the reductase:luciferase coupled reaction involves a direct channeling of FMNH₂ through two distinct mechanisms. When *V. harveyi* FRP is coupled with luciferase from *V. harveyi* or *V. fischeri*, and when *V. fischeri* FRG is coupled with luciferase from *V. fischeri*, the reduced FMNH₂ cofactor of the reductase is directly transferred to luciferase (34, 35). However, when *V. fischeri* FRG is coupled with *V. harveyi* luciferase, the reduced FMNH₂ product generated by the reductase is directly transferred to luciferase (34, 35). Hence, the mechanism of FMNH₂ transfer is dictated not unilaterally by flavin reductase or luciferase but by both constituent enzymes in the reductase:luciferase pair. A direct metabolite channeling requires a complex formation between the donor and acceptor enzyme. Indeed, the *V. harveyi* luciferase forms a complex with FRP but only with the monomeric but not the dimeric reductase (36). Such a functional complex was detected *in vitro* and *in vivo* (37). The FRP:luciferase complex formation is regulated by a balance between the FRP monomer to dimer equilibrium (K_d 1.8 μ M) and the equilibrium for luciferase and monomeric FRP binding (K_d 11 μ M) and, hence, is highly sensitive to the concentrations of FRP and luciferase. Under conditions where both the FRP:luciferase complex and free FRP and luciferase coexist, we have shown that luciferase produces bioluminescence using FMNH₂ obtained through both free diffusion and direct channeling (38). The intensity of bioluminescence derived from free-diffusing FMNH₂ can be greatly reduced by high levels of oxygen because of efficient autoxidation of the free reduced flavin whereas the light derived from directly transferred FMNH₂ is not (38).

Considering the great structural and functional diversities of the known two-component monooxygenases, it is highly unlikely that they all practice the same reduced flavin transfer mechanism. In fact, transfer through a complex formation has been reported for alkane sulfonate monooxygenase (39, 40) whereas transfer by free diffusion was observed for *Escherichia coli* (18, 41) and *Acinetobacter baumannii* (42) 4-hydroxyphenylacetate 3-monooxygenase (or *p*-hydroxyphenylacetate hydroxylase). Moreover, the *Pseudomonas putida* styrene monooxygenase system was reported to involve both free diffusion and complex formation for reduced flavin transfer (43). Catalytic efficiencies of various two-component monooxygenases should be, similar to the FRP:luciferase system, sensitive to regulations by factors such as enzyme induction mechanism, levels of enzymes and their substrates, and mechanisms and efficiencies of reduced flavin transfer.

We have been interested in the mechanisms and regulation of activity coupling between flavin reductase and luciferase for quite sometime. Tu and Hastings (44), using enzymes

from *V. harveyi* cells, reported the binding of a soluble NADH-dependent flavin reductase to immobilized luciferase. Distinct from a mixture of soluble enzymes, the time course of the bioluminescence observed with the immobilized enzyme complex was not sensitive to changes in the concentration of the enzyme sample. Moreover, for every 10-fold decrease in the concentration of luciferase plus reductase, the initial peak luminescence (at constant levels of exogenously added FMN and NADH) was reduced by 100 fold for a mixture of soluble reductase and luciferase but only by 10 fold for the immobilized enzyme complex. Therefore, the complex of immobilized luciferase and adsorbed reductase behaved as if a single enzyme species and the activity coupling between them was apparently much more efficient than a mixture of the soluble luciferase and reductase. In this study, we explore the possibility of enhancing the reduced flavin transfer in the FRP:luciferase coupled bioluminescence by generating a FRP—luciferase fusion protein. We found that the bioluminescence quantum output of one such fusion enzyme was higher without than with exogenously added FMN and, in both cases, much higher than an equal molar mixture of FRP and luciferase. More importantly, the bioluminescence of the fusion enzyme without any FMN addition was insensitive to oxygen concentration variation whereas the luminescence from a mixture of FRP and luciferase (with or without FMN addition) under similar conditions was highly diminished by increases in oxygen. These and other findings demonstrated that a fusion protein of the two constituent enzymes of a two-component monooxygenase can mimic a one-component bifunctional monooxygenase, and the coupled reaction can be catalyzed with high efficiencies by low levels of the fusion enzyme. Ordinarily FRP:luciferase can only be obtained in trace amounts because luciferase forms a complex with monomeric FRP, which can only be populated at low levels. The FRP—luciferase fusion enzyme can now be obtained at much higher levels, providing new possibilities for detailed structural and mechanistic studies that require high levels of the complex. Such an approach could be valuable to other two-component monooxygenase systems in enhancing their coupled activities under conditions hindering the efficiencies of reduced flavin transfer.

EXPERIMENTAL PROCEDURES

Materials and General Methods. All reagents were of analytical grade. FMN, bovine serum albumin, NADPH, decanal, EDTA, and protease inhibitor cocktail were from Sigma. Urea was from EM Science. IPTG, DTT, guanidine hydrochloride, T4 DNA ligase, and the Wizard SV Plus Miniprep kit were from Promega. All restriction enzymes and T4 polynucleotide kinase were from NEB. Vectors pET 28(b) and pET 21(d) were from Novagen. The Qiaex II gel extraction kit was from Qiagen. Quick Change Site-Directed Mutagenesis Kit was from Stratagene (La Jolla, CA). Oligonucleotide primers were from MWG-Biotech AG. Amicon Ultra centrifugal filter device and ultrafiltration membranes were from Millipore. DEAE-Cellulose DE-52 was from Whatman. DEAE-Sepharose resin and the HiLoad 16/60 Superdex 200 pg column were from Amersham. Lowry protein assay kit and prestained protein markers were from Bio-Rad. Unless stated otherwise, the standard buffer used throughout this study was phosphate (P_i) buffer, pH 7.0,

¹ Abbreviations: FRP, NADPH-dependent flavin reductase; FRG, NADH-NADPH utilizing general flavin reductase; DTT, dithiothreitol; EDTA, ethylenediaminetetraacetate; FMN and FMNH₂, oxidized and reduced riboflavin 5'-phosphate, respectively; FRP- $\alpha\beta$, a coisolated enzyme sample containing a fusion protein with the C-terminus of FRP fused to the N-terminus of luciferase α subunit through a 20-residue linker and a luciferase β subunit noncovalently bound to the α within the fusion protein; IPTG, isopropyl β -D-thiogalactose; LB, Luria-Bertani; PCR, polymerase chain reaction; P_i, phosphate; SDS-PAGE, sodium dodecyl sulfate—polyacrylamide gel electrophoresis; q, quantum.

consisting of mole fractions of 0.39 sodium monobase and 0.61 potassium dibase in deionized water. Sodium dodecyl sulfate–polyacrylamide gel electrophoresis (SDS–PAGE) was carried out using 10% gel. Protein concentrations were determined by the Lowry assay (45).

General Strategy for Plasmid Constructions. A three-stage procedure was followed to construct recombinant plasmids encoding FRP–luciferase fusion proteins.

Stage 1. Appending *frp* and *luxAB* Genes with Restriction Sites: A pET vector harboring the wild type *Vibrio harveyi* *frp* gene (46) was used for obtaining *frp* fragments through PCR using appropriate primer sets. Clones B, C, and D were obtained with the *frp* gene appended, respectively, with the restriction sites of *SacI/NotI*, *NdeI/BamHI*, and *SacI/NotI*, for which the first restriction site was immediately preceding the start codon and the second restriction site immediately followed the stop codon of *frp*. Clone A with *frp* appended by *NcoI/BamHI* sites was similarly obtained. However, extra GT were added between the *NcoI* site and the start codon for frame correction. Also for clones A, B, and C, the primers were designed to have the stop codon of *frp* changed to TCA for serine. Similarly, a pUC19 vector described previously (47) was used for obtaining *V. harveyi luxAB* genes through PCR using appropriate primer sets. The *luxAB* genes in clones E, F, G, and H so obtained were preceded by and followed with the restriction sites identical to those in clones A, B, C, and D, respectively. For clone E, extra GT were similarly added between the *NcoI* site and the start codon of *luxA* for frame correction. The stop codons of *luxB* in clones E, F, and G were each changed to TCA for serine. Clones C and H were selected for the construct of the fusion protein for studies reported herein (see below). The forward and reverse primers for clone C were, respectively, 5'-GAAT-TCCATATGAACAAT ACGATTGAAACCATTCTTGC-3' and 5'-CTTCGCGGATCTCTGAGCGTTTGTAGCCCC-TTACTG-3' and those for clone H were, respectively, 5'-CTTGCAGCTCATGAAATTTGGAAACTTCCTTCTCAC-3' and 5'-AAAAATGCGGCCGCTTACGAGTGGTATTT-GACGATGTTGG-3' where the restriction sites are underlined. Other primers were similarly designed.

Stage 2. Insertion of *frp* and *luxAB*: *frp* and *luxAB* genes in clones A through H described above were inserted in pairs into pET 28(b) to construct four clones by cutting and ligating with appropriate restriction enzymes. The alignments of genes in the four new recombinant plasmids (designated clones A/F, E/B, C/H, and G/D) so obtained are, respectively, ---pET28-(*NcoI*)-*frp*-(*BamHI*)---(*SacI*)-*luxA-luxB*-(*NotI*)-His₆-pET28---, ---pET28-(*NcoI*)-*luxA-luxB*-(*BamHI*)---(*SacI*)-*frp*-(*NotI*)-His₆-pET28---, ---pET28-His₆-(*NdeI*)-*frp*-(*BamHI*)---(*SacI*)-*luxA-luxB*-(*NotI*)-pET28---, and ---pET28-His₆-(*NdeI*)-*luxA-luxB*-(*BamHI*)---(*SacI*)-*frp*-(*NotI*)-pET28---, in which the restriction sites preceding and following the *frp* and *luxAB* gene are shown in parentheses, His₆ is for the His-tag sequence, and partial sequences from pET28 are shown as ---. The *frp* and *luxAB* fragments were inserted sequentially with the upstream gene inserted first.

Stage 3. Fusion of *frp* and *luxAB* with Linkers: A 20-residue peptide (sequence GS₃G₄SG₂SG₄SGAL) as the linker to fuse FRP with either the α or the β subunit of luciferase was designed following principles reported previously (48, 49). An oligomer with the corresponding sequence of 5'-GATCCTCTCTGGTGGAGGTGGATCCGGCGGTT-

CAGGTGGAGGTGGTT CTGGAGCT-3' (in which the 5' *BamHI* and the 3' *SacI* sites are underlined) was ligated to clones A/F, E/B, C/H, and G/D pretreated with *BamHI/SacI* to fuse, through the linker, *frp* with *luxA* for clones A/F and C/H and to fuse *luxB* with *frp* for clones E/B and G/D. Subsequently, extra TG bases were added after the GAGCTC *SacI* site to correct the reading frame using appropriate primer sets. When *luxA* was downstream from the *SacI* site (clones A/F, C/H), the forward and reverse primers were respectively, 5'-GGAGGTGGTTCTGGAGCTCTGATGA-AATTTGGAAACTTCC-3' and 5'-GGAAGTTTCCAAA-TTTCATCAGAGCTCCAGAACCACCTCC-3'. Similarly, when *frp* was downstream from the *SacI* site (clones E/B and G/D), the forward and reverse primers for TG insertion were 5'-GGAGGTGGTTCTGGAGCTCTGATGAACAAT ACGATTG-3' and 5'-CAATCGTATTGTTTCATCAGAGC-TCCAGAACCACCTCC-3' respectively (with *SacI* site shown as underlined and inserted TG bases in italics). The clones for all the desired fusion proteins so obtained from A/F, E/B, C/H, and G/D are designated, respectively, AF, EB, CH, and GD.

Similar to the procedures described above, clones identical to AF, EB, CH, and GD were also obtained but with FRP fused to either the luciferase α or β subunit through a 27-residue peptide linker (GS₃G₄SG₄SG₄SGAL). The identities of all clones were confirmed by nucleic acid sequencing.

Expression, Screening, and Further Cloning. Clones AF, EB, CH, and GD containing either a 20-residue or a 27-residue linker were transformed into and expressed in *Escherichia coli* BL21 cells. Cells were grown at 37 °C overnight in 50 mL of Luria–Bertani medium containing 100 μ g mL⁻¹ ampicillin and then transferred to 1 L of the same medium for further growth at the same temperature. Isopropyl 1-thio-D-galactoside (IPTG) was added up to a concentration of 0.5 mM when OD₆₀₀ reached about 0.8. The culture was grown overnight at 16 °C, and cells were harvested afterward by centrifugation.

Crude lysates of cells harboring eight different clones described above were prepared, and the FRP–luciferase coupled bioluminescence activities were determined (see below). The FRP–luciferase fusion protein contents in these crude lysates were estimated on the basis of patterns of SDS–PAGE, and specific activities of the eight lysates were estimated accordingly. We found that clones with a 20-residue linker gave better specific activities than those with a 27-residue linker, and clone CH had the highest specific activity.

To avoid any possible undesirable effects, the His tag might have on the fusion protein, the full length fusion gene from clone CH was cut with *NdeI* and *NotI* restriction enzymes and subcloned into pET 21(d) to yield a non-his tagged fusion gene. The clone so obtained, designated clone CH₂₀ (with the number of the linker residues indicated by the subscript), was used to obtain fusion enzyme for all subsequent studies. Clone CH₂₀ was transformed into *E. coli* BL21 cells, and cells were grown and harvested the same way as described above for all other clones except that 3 L of Luria–Bertani medium was used for cell growth. Clone CH₂₀ harbors the fused *frp-luxA* gene and the individual *luxB* gene. The encoded proteins, together, are referred to as FRP- $\alpha\beta$ hereafter.

Purification of FRP- $\alpha\beta$. About 20 g of cell paste was suspended in 200 mL of 50 mM P_i buffer containing 1.0 mM dithiothreitol (DTT), 1.0 mM EDTA, and 1 mL of protease inhibitor cocktail and sonicated on ice for 15–20 min. The lysed cells were centrifuged for 35 min at 12000 rpm at 4 °C. The supernatant (crude lysate) was mixed with 20 g of DEAE-cellulose DE-52 (suspended in 200 mL of 50 mM P_i buffer) and stirred for ~1 h on ice. The resin was washed by 50 mM P_i until the eluate was clear and subsequently washed with 100 mM P_i (100 mL), 200 mM P_i (100 mL), and finally eluted with 400 mM P_i buffer (~500 mL). Active fractions from the 400 mM P_i wash were collected based on the SDS-PAGE analysis and coupled activity assay. The sample obtained was diluted with cold water to 100 mM P_i buffer and loaded on a (2.5 × 25 cm) DEAE-Sepharose column pre-equilibrated with 100 mM P_i . The fusion protein was eluted with a gradient from 100 mM P_i to 500 mM P_i (500 mL) at constant flow rate of 2 mL min^{-1} . Fractions (8 mL each) containing active fusion protein were pooled and concentrated to 2 mL by ultrafiltration. This concentrated sample was then applied to a size exclusion column (16/60) Superdex 200 and eluted at 1 mL min^{-1} with 50 mM P_i containing 150 mM NaCl, 1 mM DTT and 1 mM EDTA. The enzyme sample so obtained was >95% pure on the basis of SDS-PAGE.

Enzyme Assays. All activity assays were carried out at 23 °C in standard 50 mM P_i buffer, pH 7.0. Luciferase activities were measured by a single-enzyme assay by injecting 0.5 mL of standard buffer containing 20 μM decanal and 50 μM FMN $_2$, reduced with Cu(I) (50), into an equal volume of air-saturated standard buffer containing 1 μM of free luciferase or FRP- $\alpha\beta$. Activities were measured as the peak bioluminescence intensity values (in arbitrary light unit or in qs^{-1} as specified) or, in some cases, total quantum outputs. Activities of free FRP or the FRP component in FRP- $\alpha\beta$ were also measured by a single-enzyme assay involving the measurement of $\Delta A_{340} \text{ min}^{-1}$ of a reaction solution containing designated levels of FMN, NADPH, and FRP or FRP- $\alpha\beta$. Such reactions were initiated by the addition of NADPH.

Activities of FRP- $\alpha\beta$ or an equal molar mixture of luciferase and FRP were also measured by a coupled assay method. A 10- μL aliquot of NADPH stock at a specified concentration was mixed into 1 mL standard buffer containing 25 μM FMN, 10 μM decanal, and 0.5 μM each of free luciferase and FRP or 0.5 μM FRP- $\alpha\beta$. Activities were determined as the bioluminescence peak intensity or the total quantum output.

All enzyme activity assays were performed in triplicates, and the averaged values were used for subsequent kinetic analyses. For each substrate titration curve, the activity data were fitted to the Michaelis–Menten equation and shown as the Lineweaver–Burk plot using the Prism (version 3) kinetic analysis package. The standard deviations ranged from ± 1 to $\pm 11\%$ with the median at $\pm 3.0\%$ for all triplicate sets of spectroscopic single-enzyme assays and ranged from ± 3 to $\pm 14\%$ with the median at $\pm 6\%$ for all triplicate sets of bioluminescence assays.

FMN Binding by FRP- $\alpha\beta$. FMN binding by FRP- $\alpha\beta$ was determined by quenching of the protein fluorescence at various levels of FMN addition. Excitation was set at 280 nm and emission was monitored at 330 nm using a Varian Cary Eclipse Fluorescence Spectrophotometer. Inner filter

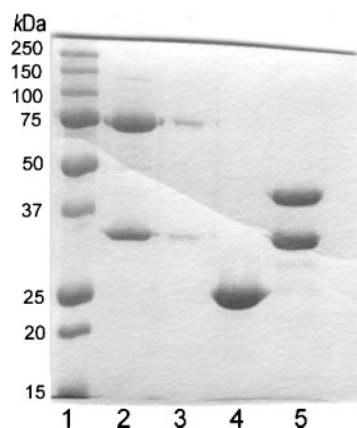


FIGURE 1: SDS-PAGE patterns for FRP- $\alpha\beta$. Lane 1, protein standards with molecular masses, in kDa, as indicated. Lanes 2 and 3, the FRP- $\alpha\beta$ fusion enzyme. Lane 4, wild type FRP. Lane 5, luciferase. A total of 10 μg protein was loaded for each of lanes 2, 4, and 5. Lane 3 was unintentionally loaded with a reduced amount of FRP- $\alpha\beta$.

effects on excitation due to high concentrations of FMN were corrected using the relationship (51)

$$F = F_{\text{obs}} \times 10^{0.5A}$$

where F and F_{obs} are, respectively, the corrected and observed fluorescence intensity, and A is the absorbance (at 1 cm light path) of the sample at the 280 nm excitation light wavelength. The samples used in this study had negligible inner filter effects on the fluorescence emission at 330 nm.

Effects of Oxygen on Bioluminescence Activity. Coupled assays using FRP- $\alpha\beta$ and a mixture of FRP and luciferase were carried out at different oxygen concentrations in standard reaction buffer. Oxygen concentration in the reaction buffer was varied as described elsewhere (38).

RESULTS

General Properties of Isolated Fusion Enzyme. SDS-PAGE analysis of the purified fusion protein showed two bands with corresponding molecular masses of 70 and 35 kDa (Figure 1, lane 2). In comparison with the FRP monomer (26.3 kDa, lane 4) and luciferase α (40.1 kDa) and β (36.3 kDa) (lane 5), the 70 kDa band of the purified fusion enzyme corresponded to the fused FRP- α species, as expected, and the 35 kDa band corresponded to the luciferase β that was noncovalently bound by and co-isolated with FRP- α . No protein bands corresponding to luciferase α or FRP monomer were detected. The identity of the isolated fusion enzyme as FRP- $\alpha\beta$ was thus confirmed.

FRP is known to have one FMN cofactor site per 26.3 kDa monomer (52). The isolated FRP- $\alpha\beta$ was yellow in color, with an absorption spectrum essentially the same as that for FRP (Figure 2). On the basis of the known extinction coefficient at 453 nm of FRP-bound FMN (32), an FRP sample isolated in this study showed 0.78 bound FMN per monomer whereas the fusion enzyme had 0.42 bound FMN per FRP- $\alpha\beta$ (Figure 2). Since 58% of the isolated FRP- $\alpha\beta$ did not contain any bound FMN, its ability to bind exogenously added FMN was tested by following protein fluorescence quenching of a limiting amount of FRP- $\alpha\beta$ upon FMN titration. The protein fluorescence gradually decreased at increasing FMN concentrations (Figure 3A). Double

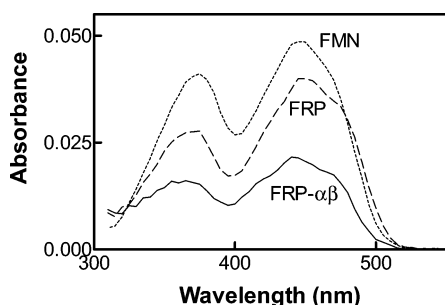


FIGURE 2: Absorption spectrum of FRP- $\alpha\beta$. Absorption spectrum of a purified sample of fusion protein FRP- $\alpha\beta$ at 5 μM was recorded in 50 mM Pi buffer, pH 7.0, in a 1-cm path length cuvette (—). For comparison, absorption spectra of FRP (---) and FMN (····) were also obtained at the same concentration.

reciprocal plot of $\Delta\text{Fluorescence}$ versus FMN concentration gave rise to a linear line consistent with a K_d of $24 \pm 2 \mu\text{M}$ (Figure 3B).

Activities of FRP- $\alpha\beta$. The enzymatic activities of FRP- $\alpha\beta$ in comparison with free FRP and luciferase in single-enzyme assays and coupled bioluminescence assays are summarized in Table 1. In single-enzyme bioluminescence assays measuring peak intensities, the luciferase component of FRP- $\alpha\beta$ was found to have a specific activity of $(1.1 \pm 0.1) \times 10^{13} \text{ qs}^{-1} \text{ nmol}^{-1}$, making it 92% as active as wild type luciferase sample tested under same conditions. By measuring $\Delta A_{340} \text{ min}^{-1}$ in single-enzyme assays using 60 μM FMN and 200 μM NADPH, the FRP component of FRP- $\alpha\beta$ gave rise to a k_{cat} of 700 min^{-1} , rendering it about 31% as active as wild type FRP sample (k_{cat} of 2250 min^{-1}). The activity of FRP- $\alpha\beta$ (at 0.5 μM) was also compared with a mixture of FRP and luciferase (each at 0.5 μM) in coupled bioluminescence assays using 200 μM NADPH, 25 μM FMN, and 10 μM decanal. On the basis of peak bioluminescence intensities, FRP- $\alpha\beta$ showed an activity of $6.0 \times 10^{12} \text{ qs}^{-1} \text{ nmol}^{-1}$, which was 63% as active as a mixture of luciferase and FRP assayed under identical conditions.

Steady-State Kinetics Analyses. Using the FRP single-enzyme spectrophotometric assay, double reciprocal plots of initial velocities versus concentrations of FMN as the varying substrate at several fixed levels of NADPH (Figure 4A) or NADPH as the varying substrate at several concentrations of FMN (Figure 4B) gave, in each case, a set of parallel lines, indicating the same ping-pong mechanism reported previously for free FRP (34, 53). In secondary plots of ordinate intercepts versus $1/[\text{NADPH}]$ (from Figure 4A) and $1/[\text{FMN}]$ (from Figure 4B), linear lines were obtained, allowing the determination of $310 \pm 30 \mu\text{M}$ for $K_{\text{m,NADPH}}$, $72 \pm 15 \mu\text{M}$ for $K_{\text{m,FMN}}$ and, by extrapolation to infinite substrate concentrations, $710 \pm 55 \text{ min}^{-1}$ for k_{cat} (Table 1). The k_{cat} so obtained was similar to the value of 700 min^{-1} determined at a fixed high concentration for each of FMN (60 μM) and NADPH (200 μM) as reported above. Both K_{m} values were considerably higher than the corresponding 20 μM $K_{\text{m,NADPH}}$ and 8 μM $K_{\text{m,FMN}}$ for free FRP (34).

The coupled bioluminescence assay was also used to determine the activities of FRP- $\alpha\beta$ using FMN as the varying substrate at several fixed levels of NADPH (Figure 5A) and with NADPH as the varying substrate at several constant FMN concentrations (Figure 5B). In both cases, reciprocal plots of peak bioluminescence intensities versus concentrations of the varying substrate showed a series of converging

lines, consistent with a sequential mechanism same as that reported for the coupled reaction using a mixture of luciferase and FRP (34). Secondary plots were constructed for ordinate intercepts and slopes versus reciprocal of NADPH concentrations (data taken from Figure 5A). Linear plots were obtained, giving rise to $K_{\text{m,NADPH}}$ of $6.6 \pm 0.5 \mu\text{M}$, $K_{\text{m,FMN}}$ of $0.93 \pm 0.45 \mu\text{M}$, and V_{max} of $(6.9 \pm 0.1) \times 10^{12} \text{ qs}^{-1} \text{ nmol}^{-1}$ (Table 1). The V_{max} so obtained by extrapolation to infinite FMN and NADPH was slightly higher than the $6.0 \times 10^{12} \text{ qs}^{-1} \text{ nmol}^{-1}$ observed at a fixed 25 μM FMN and 200 μM NADPH as mentioned above. The K_{m} values for NADPH and FMN for FRP- $\alpha\beta$ in the coupled reaction were considerably lower than the corresponding K_{m} values determined in the FRP single-enzyme assays. This characteristic is similar to that reported for FRP and the coupled reaction using a mixture of FRP and luciferase (34). However, quantitatively the $K_{\text{m,FMN}}$ and, especially, $K_{\text{m,NADPH}}$ of FRP- $\alpha\beta$ in the coupled reaction were higher than the corresponding $K_{\text{m,FMN}}$ of 0.3 μM and $K_{\text{m,NADPH}}$ of 0.02 μM for the coupled reaction using a mixture of FRP and luciferase (34).

Total Quantum Outputs. The total quantum output of FRP- $\alpha\beta$ (tested at 0.1 μM) using 10 μM decanal and 5 μM NADPH without any FMN addition was determined to be $(8.1 \pm 0.9) \times 10^{12} \text{ q}$, a level 22% higher than that for FRP- $\alpha\beta$ in the presence of 25 μM exogenously added FMN (Figure 6). Under the same reaction conditions but with a mixture of FRP and luciferase (each at 0.1 μM) replacing FRP- $\alpha\beta$, the total quantum outputs were found to be similar either without or with the addition of 25 μM FMN. Moreover, both were only about 7% of that for FRP- $\alpha\beta$ without any added FMN (Figure 6).

Effects of Oxygen on Light Intensities of Coupled Bioluminescence Reaction. At 0.5 μM FRP- $\alpha\beta$ without any addition of FMN, the light intensity was found to remain at a constant level of $2.3 \times 10^{12} \text{ qs}^{-1}$ over the range of 0.12 to 1.28 mM of oxygen (Figure 7A, \blacktriangle). With the addition of 25 μM FMN, the highest intensity ($6 \times 10^{12} \text{ qs}^{-1}$) was observed at the lowest oxygen concentration (0.12 mM) tested, and increases of oxygen level resulted in gradual decreases in bioluminescence intensity to a final level near zero (Figure 7A, \bullet). For a mixture of luciferase and FRP (each at 0.5 μM), light intensities at the lowest O_2 concentration of 0.12 mM were found at levels of $8.2 \times 10^{10} \text{ qs}^{-1}$ and $5 \times 10^{11} \text{ qs}^{-1}$ for samples with the addition of zero and 25 μM FMN, respectively (Figure 7B). In both cases, increases in oxygen concentration led to marked decreases in bioluminescence intensity in similar patterns (Figure 7B).

DISCUSSION

The isolated fusion enzyme was yellow in color due to bound FMN at a molar ratio of about 0.42 FMN per FRP- $\alpha\beta$ (Figure 2). The FMN cofactor binding affinity by this 42% holoenzyme subpopulation of the isolated FRP- $\alpha\beta$ was not determined but was apparently high, similar to that by the apoenzyme of the wild-type FRP (K_d of 0.2 μM at 23 $^\circ\text{C}$) (52). The other 58% of the FMN-free subpopulation of FRP- $\alpha\beta$ was able to bind exogenously added FMN with a K_d of 24 μM at 23 $^\circ\text{C}$ (Figure 3). This binding affinity was much stronger than that by wild type luciferase (K_d 373 μM) at 24 $^\circ\text{C}$ (54). The observed binding of exogenously added FMN was highly unlikely by the luciferase component of

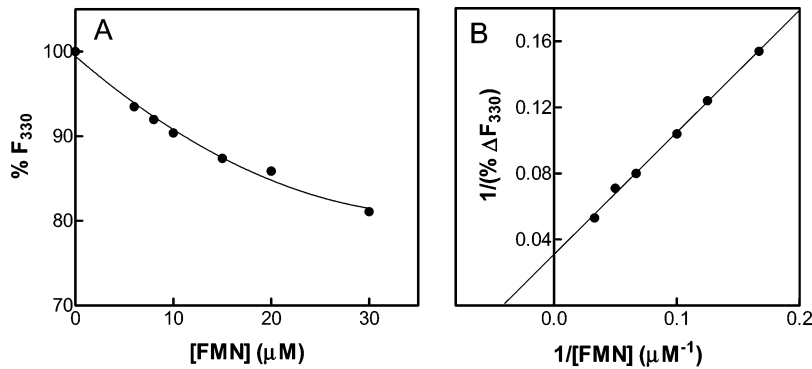


FIGURE 3: Fluorometric titrations of FRP- $\alpha\beta$ with FMN. (A) A constant amount of FRP- $\alpha\beta$ at $1\ \mu\text{M}$ in $50\ \text{mM}$ Pi was titrated with FMN at levels as indicated. Emission intensities at $330\ \text{nm}$ were measured using an excitation at $280\ \text{nm}$, and normalized fluorescence intensities are plotted against FMN concentrations. Observed fluorescence intensities were corrected for inner filter effect of FMN on excitation as described in the Experimental Procedures. (B) Normalized $\Delta\text{Fluorescence}$, defined as the difference of the emission intensity of FRP- $\alpha\beta$ minus that with the addition of a given amount of flavin, is plotted against FMN concentrations. Data are shown as a double reciprocal plot.

Table 1: Comparison of Kinetic Parameters of FRP- $\alpha\beta$ with FRP and Luciferase under Various Assay Conditions

enzyme sample	activity/assay method	k_{cat} or V_{max}	$K_{\text{m,FMN}}\ (\mu\text{M})$	$K_{\text{m,NADPH}}\ (\mu\text{M})$
luciferase	luciferase/bioluminescence	$(1.2 \pm 0.1) \times 10^{13}\ \text{qs}^{-1}\ \text{nmol}^{-1}$		
FRP- $\alpha\beta$	luciferase/bioluminescence	$(1.1 \pm 0.1) \times 10^{13}\ \text{qs}^{-1}\ \text{nmol}^{-1}$		
FRP ^a	FRP/spectrophotometric	$2250\ \text{min}^{-1}$	8	20
FRP- $\alpha\beta$	FRP/spectrophotometric	$710 \pm 55\ \text{min}^{-1}$	72 ± 15	310 ± 30
FRP ^a	FRP/luciferase-coupled	$9.5 \times 10^{12}\ \text{qs}^{-1}\ \text{nmol}^{-1}$	0.3	0.02
FRP- $\alpha\beta$	FRP/luciferase-coupled	$(6.9 \pm 0.1) \times 10^{12}\ \text{qs}^{-1}\ \text{nmol}^{-1}$	0.93 ± 0.45	6.6 ± 0.5

^a Data taken from ref 34.

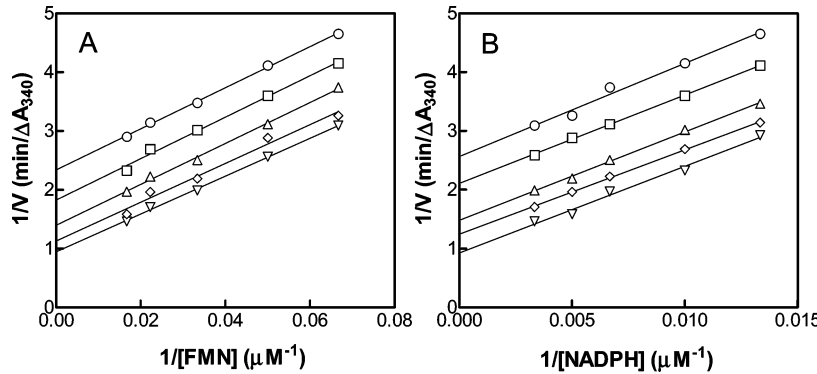


FIGURE 4: Steady-state kinetic analyses of FRP- $\alpha\beta$ as a function of substrate concentration using FRP single enzyme spectrophotometric assay. (A) Double reciprocal plots of initial velocity (v) as a function of FMN concentration at constant levels of $75\ (\bigcirc)$, $100\ (\square)$, $150\ (\triangle)$, $200\ (\diamond)$, and $300\ \mu\text{M}\ (\nabla)$ NADPH. (B) Double reciprocal plots of initial velocity as a function of NADPH concentration at constant levels of $15\ (\bigcirc)$, $20\ (\square)$, $30\ (\triangle)$, $45\ (\diamond)$, and $60\ \mu\text{M}\ (\nabla)$ FMN.

FRP- $\alpha\beta$ and, hence, was attributed to the 58% of the FRP component of the isolated FRP- $\alpha\beta$ that was originally without bound flavin. Furthermore, we favor the interpretation that the 42% holoenzyme subpopulation of the isolated FRP- $\alpha\beta$ was catalytically active whereas the other 58% FMN-free subpopulation of FRP- $\alpha\beta$ was catalytically either inactive or very weakly active. This was supported by the findings that activities of FRP- $\alpha\beta$ showed normal Michaelis–Menton kinetic patterns during FMN titrations over a range of 5 to $60\ \mu\text{M}$ (Figures 4, 5).

Both the FRP and the luciferase components of the FRP- $\alpha\beta$ fusion enzyme retained rather good catalytic activities. On the basis of luciferase single-enzyme assay, FRP- $\alpha\beta$ had a specific activity of $1.1 \pm 0.1 \times 10^{13}\ \text{qs}^{-1}\ \text{nmol}^{-1}$, which was 92% of that for the wild type luciferase. By the use of the FRP spectrophotometric assay, the k_{cat} of FRP- $\alpha\beta$ ($710\ \text{min}^{-1}$) was about 31% of that for wild type FRP. Following our notion that only 42% of the holoenzyme portion of the

isolated FRP- $\alpha\beta$ was catalytically active, the specific activity of the holoenzyme subpopulation of FRP- $\alpha\beta$ could be as high as 74% as the wild-type FRP. Under our experimental conditions for coupled bioluminescence assays using a fixed high concentration for each of FMN and NADPH, FRP- $\alpha\beta$ was found to be about $6.0 \times 10^{12}\ \text{qs}^{-1}\ \text{nmol}^{-1}$ or 63% active as an equal molar mixture of luciferase and FRP. The true V_{max} obtained by substrate titrations in coupled bioluminescence assays (Figure 4 and subsequent secondary plots) gave rise to a value of $6.9 \pm 0.1 \times 10^{12}\ \text{qs}^{-1}\ \text{nmol}^{-1}$ for FRP- $\alpha\beta$, equivalent to 73% of the V_{max} for an equal molar mixture of FRP and luciferase. Taken all activity measurements together, FRP- $\alpha\beta$ was quite good as a fusion enzyme.

Early on, the optimal FMN concentration for the NADH/NADPH-utilizing flavin reductase FRG from *Vibrio fischeri* in luciferase-coupled bioluminescence reaction was found about 100 times lower than that in the reductase single-enzyme spectrophotometric assay (55). More detailed studies

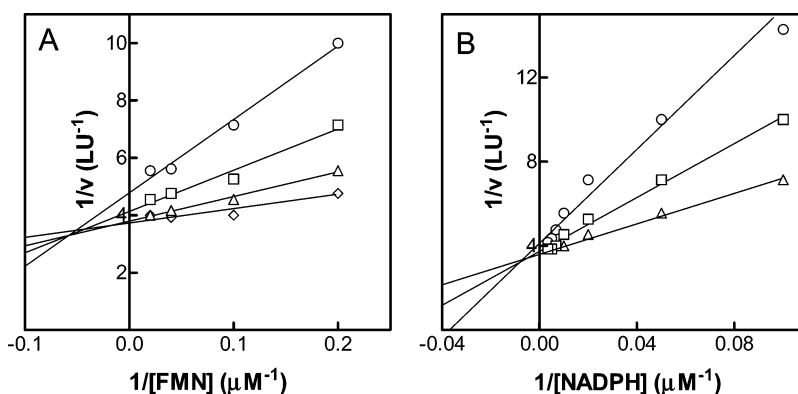


FIGURE 5: Steady-state kinetic analyses of fusion protein FRP- $\alpha\beta$ as a function of substrate concentration using coupled assay. (A) Double reciprocal plots of initial velocity (v) as a function of FMN concentration at constant levels of 20 (\circ), 50 (\square), 100 (\triangle) and 150 μM (\diamond) NADPH. (B) Double reciprocal plots of initial velocity (v) as a function of NADPH concentration at constant levels of 5 (\circ), 10 (\square) and 50 μM (\triangle) FMN.

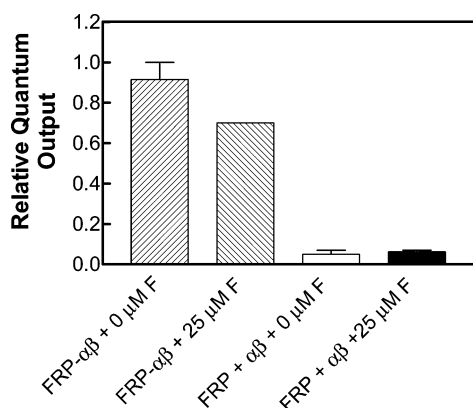
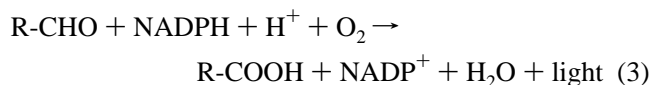


FIGURE 6: Comparison of quantum yields of FRP- $\alpha\beta$ and an equal molar mixture of FRP and luciferase. Coupled bioluminescence reactions were carried out using 0.1 μM FRP- $\alpha\beta$ or a mixture of FRP and luciferase with each at 0.1 μM . In addition to the enzyme sample, the 1-mL reaction solution also contained 5 μM NADPH, 10 μM decanal, and either zero or 25 μM additionally added FMN. Bioluminescence emissions were allowed to reach completion, and the total quanta outputs were determined. Quantum yield was determined as the number of quanta emitted per molecule of NADPH consumed.

on *V. harveyi* FRP and luciferase subsequently showed that the $K_{m,\text{FMN}}$ and $K_{m,\text{NADPH}}$ for FRP in the coupled bioluminescence reaction were markedly lower than that determined by FRP single-enzyme assay (34, 35, 53). These findings indicate a direct FMNH₂ transfer from reductase to luciferase within an active complex of the two enzymes (34). As single enzymes, flavin reductases have much faster turnover rates than luciferases. It was reasoned that, at substrate levels much lower than the K_m s for reductase single-enzyme reaction, the reductase within the active complex can already supply sufficient FMNH₂ to enable 50% V_{max} of luciferase within the same complex, thus resulting in apparently much lower K_m values in luciferase-coupled reactions (34). This important characteristic for direct FMNH₂ transfer was similarly observed for FRP- $\alpha\beta$, which showed 6.6 μM $K_{m,\text{NADPH}}$ and 0.93 μM $K_{m,\text{FMN}}$ in the coupled bioluminescence reaction, much lower than the corresponding 310 μM $K_{m,\text{NADPH}}$ and 72 μM $K_{m,\text{FMN}}$ determined by the FRP spectrophotometric assay. Another important characteristic supporting a direct transfer of reduced flavin cofactor rather than reduced flavin product by FRP is the shift from a ping-pong mechanism for FRP as a single enzyme to a sequential kinetic pattern

for the FRP:luciferase coupled bioluminescence reaction (34, 35). This feature was also maintained by the FRP- $\alpha\beta$ fusion enzyme (Figures 4, 5). The construct of the FRP- $\alpha\beta$ fusion enzyme apparently did not change, qualitatively, any of the key characteristics with respect to FMNH₂ transfer from FRP and luciferase.

Interestingly, FRP- $\alpha\beta$ was found to differ from a mixture of luciferase and FRP in two important aspects of the coupled bioluminescence reaction. First, the total quantum outputs of the coupled bioluminescence reaction catalyzed by FRP- $\alpha\beta$, at 0.1 μM , were considerably higher than those by an equal molar mixture of luciferase and FRP under similar conditions (Figure 6). Of particular importance is the finding that the total quantum output observed with FRP- $\alpha\beta$ was higher without than with the addition of 25 μM FMN (Figure 6). For the bioluminescence to occur in the coupled reaction, the luciferase component of FRP- $\alpha\beta$ must receive FMNH₂ produced by the FRP component. Without any exogenously added FMN, the coupled bioluminescence reaction solution contained a total of 0.04 μM FMN originally bound by the 0.1 μM FRP- $\alpha\beta$. Even at this low level, the FMN apparently was retained by the FRP component of FRP- $\alpha\beta$ to react with NADPH for the production of FMNH₂, which was in turn utilized directly by the luciferase component for bioluminescence. The overall reaction can be expressed as:



FRP- $\alpha\beta$ relied on and can retain the originally bound FMN to catalyze such a reaction. Therefore, FRP- $\alpha\beta$ mimics a single-component bifunctional monooxygenase in catalyzing the overall reaction without flavin addition.

A second unusual aspect of the FRP- $\alpha\beta$ -catalyzed coupled bioluminescence was related to the effects of oxygen concentration on bioluminescence intensity. Oxygen can compete against luciferase in reacting with the free-diffusing FMNH₂ through autoxidation whereas the FMNH₂ directly transferred to luciferase through a complex with FRP is not sensitive to autoxidation. Under conditions that the FRP:luciferase complex and free FRP and luciferase coexist, we have shown that the observed bioluminescence is derived from FMNH₂ obtained by luciferase through both diffusion and direct channeling (38). By using a mixture of FRP and

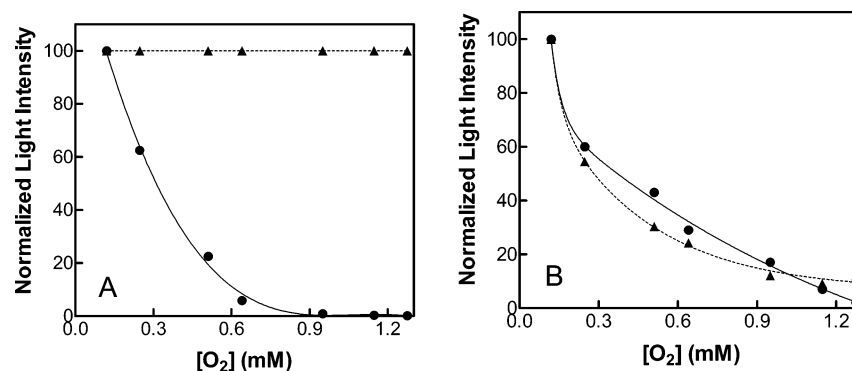


FIGURE 7: Effects of oxygen on light intensities of coupled bioluminescence reactions catalyzed by FRP- $\alpha\beta$ or an equal molar mixture of FRP and luciferase. Effects of oxygen concentration on the peak light intensity in the coupled bioluminescence reaction were examined for 0.5 μM FRP- $\alpha\beta$ (panel A) and a mixture of equal molar luciferase plus FRP (each at 0.5 μM) (panel B) with the addition of 200 μM NADPH, 10 μM decanal, and zero (▲) or 25 μM (●) FMN. For panel A, the highest bioluminescence intensities observed without and with the addition of 25 μM FMN were, respectively, 2.3×10^{12} and 6×10^{12} qs^{-1} . For panel B, the highest bioluminescence intensities observed without and with the addition of 25 μM FMN were, respectively, 8.2×10^{10} and 5×10^{11} qs^{-1} . In each case, the highest intensity was normalized to 100, and all other intensities were normalized accordingly for presentation.

luciferase (each at a low level of 0.5 μM) with and without the addition of 25 μM FMN, intensities of the coupled bioluminescence were in both cases gradually reduced to close to zero as the O₂ increased from 0.12 to 1.28 mM (Figure 7B). These findings indicated that the observed bioluminescence was nearly entirely derived from the free-diffusing FMNH₂ because of a lack of significant formation of FRP:luciferase complex on the basis of known binding equilibrium constant (K_d 11 μM) (36). In a sharp contrast, the bioluminescence catalyzed by 0.5 μM FRP- $\alpha\beta$ without any exogenously added FMN was insensitive to increasing levels of oxygen (Figure 7A), indicating a high efficiency for direct transfer of FMNH₂ within the fusion enzyme. Once again, such a finding strongly supports the conclusion that FRP- $\alpha\beta$ is able to mimic a single-component bifunctional monooxygenase.

The flavin cofactor of FRP apparently shuffled between FRP and luciferase within the FRP- $\alpha\beta$ fusion enzyme. In this connection, the single-component *p*-hydroxybenzoate hydroxylase has been shown and other genuine single-component bifunctional monooxygenases are also likely to involve significant protein and flavin dynamic movements between an “in” and an “open” conformation during catalysis (56, 57). The dynamics of the flavin cofactor in FRP- $\alpha\beta$ during catalysis could be different in details from that of genuine single-component bifunctional monooxygenases, but the essentiality of flavin dynamics in catalysis appears to be a common feature. It should also be noted that, interestingly, the two-component *p*-hydroxyphenylacetate hydroxylase from *A. baumannii* has recently been shown to rely on rapid diffusion of reduced flavin from reductase to monooxygenase for activity without any exogenously added flavin (42). Apparently, the reduced flavin also shuttled between the two constituent enzymes of this two-component monooxygenase during catalysis.

Figure 7A shows that the light intensity of the coupled reaction catalyzed by FRP- $\alpha\beta$ with the addition of 25 μM FMN also gradually decreased to near zero at increasing oxygen concentrations. We believe that, because of the ping-pong type of FRP activity, the exogenously added FMN can compete against luciferase in reacting with the reduced FMNH₂ cofactor bound to the FRP component of the fusion enzyme to form the FMNH₂ product. The reduced flavin

product so generated can still be utilized by luciferase for bioluminescence through diffusion but is sensitive to autooxidation at high O₂ levels, resulting in much reduced bioluminescence emission. This type of “stealing” of reducing equivalent from the reduced flavin cofactor of salicylate hydroxylase, a single-component bifunctional monooxygenase, by exogenously added oxidized flavin has also been shown to result in the uncoupling of NADH oxidation (hence flavin cofactor reduction) from substrate monooxygenation (58).

An increasing number of two-component monooxygenase couples have been identified in recent years. As already described in Introduction, diverse mechanisms have been revealed for reduced flavin transfer by the several two-component monooxygenase systems investigated thus far. For FRP:luciferase and other two-component monooxygenases, the efficiencies of reduced flavin transfer *in vitro* and *in vivo* should all be quite sensitive to variations of concentrations of the enzymes, NAD(P)H, flavin, hydroxylatable substrate, and oxygen. We have shown that the FRP- $\alpha\beta$ fusion enzyme mimics a single-component bifunctional monooxygenase, exhibiting efficient coupled bioluminescence activities without any exogenously added flavin by relying on a shuffling of flavin between FRP and luciferase within the fusion protein. Our findings suggest that the same approach could be useful in converting other two-component monooxygenase couples to fused single-component bifunctional monooxygenases. Such “clubbing” together of adjacent enzymes in biochemical pathways is also of particular advantage, in plants and other higher organisms with complicated gene expression and regulatory systems, in what is called metabolic engineering. Two or more consecutive enzymes can be fused for constructing single multigene expression cassettes to facilitate gene expression, eliminate need for multiple co-transformations, and overcome gene silencing (59).

Luciferase forms a complex with the FRP monomer but not the dimer. Because of the 2 μM K_d for FRP monomer–dimer equilibrium, FRP monomers can only be efficiently populated at sub-micromolar levels. Consequently, the FRP:luciferase complex can only be obtained at low levels as well. This presents a major obstacle for any studies that require higher concentrations of the FRP:luciferase complex.

The FRP- $\alpha\beta$ fusion enzyme can be isolated at levels of tens of micromolar or higher. Therefore, this fusion enzyme should also be invaluable for studies that cannot be performed with low levels of the noncovalent complex of FRP: luciferase.

Bacterial luciferases provide an invaluable tool as *in vitro* and *in vivo* reporters for a great number of basic and applied researches in life sciences (60, 61). Low levels of luciferase expression and/or low efficiencies for the provision of FMNH₂ to luciferase could be a major obstacle for such applications. The use of FRP- $\alpha\beta$ instead of free luciferase as a reporter could be beneficial, especially when expressions are low.

ACKNOWLEDGMENT

We thank Dr. Uli Strych for his inputs in cloning.

REFERENCES

- Ziegler, D. M. (2002) An overview of the mechanism, substrate specificities, and structure of FMOs, *Drug Metab. Rev.* 34, 503–511.
- Cole, L. J., Entsch, B., Ortiz-Maldonado, M., and Ballou, D. P. (2005) Properties of *p*-hydroxybenzoate hydroxylase when stabilized in its open conformation, *Biochemistry* 44, 14807–14817.
- Wang, L.-H., and Tu, S.-C. (1984) The kinetic mechanism of salicylate hydroxylase as studied by initial rate measurement, rapid reaction kinetics, and isotope effects, *J. Biol. Chem.* 259, 10682–10688.
- Yu, Y., Wang, L.-H., and Tu, S.-C. (1987) *Pseudomonas cepacia* 3-hydroxybenzoate 6-hydroxylase: stereochemistry, isotope effects, and kinetic mechanism, *Biochemistry* 26, 1105–1110.
- Tu, S.-C. (2001) Reduced flavin: donor and acceptor enzymes and mechanisms of channeling, *Antioxid. Redox Signal.* 3, 881–897.
- van Berkel, W. J., Kamerbeek, N. M., and Fraaije, M. W. (2006) Flavoprotein monooxygenases, a diverse class of oxidative biocatalysts, *J. Biotechnol.* 124, 670–689.
- Hastings, J. W., and Nealson, K. H. (1977) Bacterial bioluminescence, *Annu. Rev. Microbiol.* 31, 549–595.
- Lei, B., and Tu, S.-C. (1996) Gene overexpression, purification, and identification of a desulfurization enzyme from *Rhodococcus* sp. strain IGTS8 as a sulfide/sulfoxide monooxygenase, *J. Bacteriol.* 178, 5699–5705.
- Gray, K. A., Pogrebinsky, O. S., Mrachko, G. T., Xi, L., Monticello, D. J., and Squires, C. H. (1996) Molecular mechanisms of biocatalytic desulfurization of fossil fuels, *Nat. Biotechnol.* 14, 1705–1709.
- Kendrew, S. G., Hopwood, D. A., and Marsh, E. N. (1997) Identification of a monooxygenase from *Streptomyces coelicolor* A3(2) involved in biosynthesis of actinorhodin: purification and characterization of the recombinant enzyme, *J. Bacteriol.* 179, 4305–4310.
- Valton, J., Filisetti, L., Fontecave, M., and Nivière, V. (2004) A two-component flavin-dependent monooxygenase involved in actinorhodin biosynthesis in *Streptomyces coelicolor*, *J. Biol. Chem.* 279, 44362–44369.
- Blanc, V., Lagneaux, D., Didier, P., Gil, P., Lacroix, P., and Crouzet, J. (1995) Cloning and analysis of structural genes from *Streptomyces pristinaespiralis* encoding enzymes involved in the conversion of pristinamycin IIB to pristinamycin IIA (PIIA): PIIA synthase and NADH:riboflavin 5'-phosphate oxidoreductase, *J. Bacteriol.* 177, 5206–5214.
- Thibaut, D., Ratet, N., Bisch, D., Faucher, D., Debussche, L., and Blanche, F. (1995) Purification of the two-enzyme system catalyzing the oxidation of the D-proline residue of pristinamycin IIB during the last step of pristinamycin IIA biosynthesis, *J. Bacteriol.* 177, 5199–5205.
- Parry, R. J., and Li, W. (1997) Purification and characterization of isobutylamine N-hydroxylase from the valanimycin producer *Streptomyces viridifaciens* MG456-hF10, *Arch. Biochem. Biophys.* 339, 47–54.
- Arunachalam, U., Massey, V., and Vaidyanathan, C. S. (1992) *p*-Hydroxyphenylacetate-3-hydroxylase. A two-protein component enzyme, *J. Biol. Chem.* 267, 25848–25855.
- Chaiyen, P., Suadee, C., and Wilairat, P. (2001) A novel two-protein component flavoprotein hydroxylase, *Eur. J. Biochem.* 268, 5550–5561.
- Prieto, M. A., and Garcia, J. L. (1994) Molecular characterization of 4-hydroxyphenylacetate 3-hydroxylase of *Escherichia coli*. A two-protein component enzyme, *J. Biol. Chem.* 269, 22823–22829.
- Louie, T. M., Xie, X. S., and Xun, L. (2003) Coordinated production and utilization of FADH₂ by NAD(P)H-flavin oxidoreductase and 4-hydroxyphenylacetate 3-monooxygenase, *Biochemistry* 42, 7509–7517.
- Becker, D., Schrader, T., and Andreesen, J. R. (1997) Two-component flavin-dependent pyrrole-2-carboxylate monooxygenase from *Rhodococcus* sp., *Eur. J. Biochem.* 249, 739–747.
- Xu, Y., Mortimer, M. W., Fisher, T. S., Kahn, M. L., Brockman, F. J., and Xun, L. (1997) Cloning, sequencing, and analysis of a gene cluster from *Chelatobacter heintzii* ATCC 29600 encoding nitrilotriacetate monooxygenase and NADH:flavin mononucleotide oxidoreductase, *J. Bacteriol.* 179, 1112–1116.
- Uetz, T., Schneider, R., Snozzi, M., and Egli, T. (1992) Purification and characterization of a two-component monooxygenase that hydroxylates nitrilotriacetate from "Chelatobacter" strain ATCC 29600, *J. Bacteriol.* 174, 1179–1188.
- Russell, T. R., Demeler, B., and Tu, S.-C. (2004) Kinetic mechanism and quaternary structure of *Aminobacter aminovorans* NADH:flavin oxidoreductase: an unusual flavin reductase with bound flavin, *Biochemistry* 43, 1580–1590.
- Payne, J. W., Bolton, H., Jr., Campbell, J. A., and Xun, L. (1998) Purification and characterization of EDTA monooxygenase from the EDTA-degrading bacterium BNC1 [published erratum appears in J Bacteriol 1998 Nov;180(21):5808], *J. Bacteriol.* 180, 3823–3827.
- Witschel, M., Nagel, S., and Egli, T. (1997) Identification and characterization of the two-enzyme system catalyzing oxidation of EDTA in the EDTA-degrading bacterial strain DSM 9103, *J. Bacteriol.* 179, 6937–6943.
- Gisi, M. R., and Xun, L. (2003) Characterization of chlorophenol 4-monooxygenase (TftD) and NADH:flavin adenine dinucleotide oxidoreductase (TftC) of *Burkholderia cepacia* AC1100, *J. Bacteriol.* 185, 2786–2792.
- Garrec, G. M., Artaud, I., and Capeillère-Blandin, C. (2001) Purification and catalytic properties of the chlorophenol 4-monooxygenase from *Burkholderia cepacia* strain AC1100, *Biochim. Biophys. Acta* 1547, 288–301.
- Pessione, E., Divari, S., Griva, E., Cavaletto, M., Rossi, G. L., Gilardi, G., and Giunta, C. (1999) Phenol hydroxylase from *Acinetobacter radioresistens* is a multicomponent enzyme. Purification and characterization of the reductase moiety, *Eur. J. Biochem.* 265, 549–555.
- Kirchner, U., Westphal, A. H., Mueller, R., and Van Berkel, W. J. H. (2003) Phenol hydroxylase from *Bacillus thermoglucosidans* A7, a two-protein component monooxygenase with a dual Role for FAD, *J. Biol. Chem.* 278, 47545–47553.
- Divari, S., Valetti, F., Caposio, P., Pessione, E., Cavaletto, M., Griva, E., Gribaudo, G., Gilardi, G., and Giunta, C. (2003) The oxygenase component of phenol hydroxylase from *Acinetobacter radioresistens* S13, *Eur. J. Biochem.* 270, 2244–2253.
- Eichhorn, E., van der Ploeg, J. R., and Leisinger, T. (1999) Characterization of a two-component alkanesulfonate monooxygenase from *Escherichia coli*, *J. Biol. Chem.* 274, 26639–26646.
- Otto, K., Hofstetter, K., Rothlisberger, M., Witholt, B., and Schmid, A. (2004) Biochemical characterization of StyAB from *Pseudomonas* sp. strain VLB120 as a two-component flavin-diffusible monooxygenase, *J. Bacteriol.* 186, 5292–5302.
- Lei, B., Liu, M., Huang, S., and Tu, S.-C. (1994) *Vibrio harveyi* NADPH-flavin oxidoreductase: cloning, sequencing and overexpression of the gene and purification and characterization of the cloned enzyme, *J. Bacteriol.* 176, 3552–3558.
- Inouye, S. (1994) NAD(P)H-flavin oxidoreductase from the bioluminescent bacterium, *Vibrio fischeri* ATCC 7744, is a flavoprotein, *FEBS Lett.* 347, 163–168.
- Lei, B., and Tu, S.-C. (1998) Mechanism of reduced flavin transfer from *Vibrio harveyi* NADPH-FMN oxidoreductase to luciferase, *Biochemistry* 37, 14623–14629.

35. Jeffers, C. E., and Tu, S.-C. (2001) Differential transfers of reduced flavin cofactor and product by bacterial flavin reductase to luciferase, *Biochemistry* 40, 1749–1754.
36. Jeffers, C. E., Nichols, J. C., and Tu, S.-C. (2003) Complex formation between *Vibrio harveyi* luciferase and monomeric NADPH:FMN oxidoreductase, *Biochemistry* 42, 529–534.
37. Low, J. C., and Tu, S.-C. (2003) Energy transfer evidence for *in vitro* and *in vivo* complexes of *Vibrio harveyi* flavin reductase P and luciferase, *Photochem. Photobiol.* 77, 446–452.
38. Li, X., and Tu, S.-C. (2006) Activity Coupling of *Vibrio harveyi* luciferase and flavin reductase (FRP): Oxygen as a probe, *Arch. Biochem. Biophys.* 454, 26–31.
39. Gao, B., and Ellis, H. R. (2005) Altered mechanism of the alkanesulfonate FMN reductase with the monooxygenase enzyme, *Biochem. Biophys. Res. Commun.* 331, 1137–1145.
40. Abdurachim, K., and Ellis, H. R. (2006) Detection of protein-protein interactions in the alkanesulfonate monooxygenase system from *Escherichia coli*, *J. Bacteriol.* 188, 8153–8159.
41. Galán, B., Díaz, E., Prieto, M. A., and García, J. L. (2000) Functional analysis of the small component of the 4-hydroxyphenylacetate 3-monooxygenase of *Escherichia coli* W: a prototype of a new flavin:NAD(P)H reductase subfamily, *J. Bacteriol.* 182, 627–636.
42. Sucharitakul, J., Phongsak, T., Entsch, B., Svasti, J., Chaiyen, P., and Ballou, D. P. (2007) Kinetics of a two-component *p*-hydroxyphenylacetate hydroxylase explain how reduced flavin is transferred from the reductase to the oxygenase, *Biochemistry*, DOI: 10.1021/bi7006614.
43. Kantz, A., Chin, F., Nallamothu, N., Nguyen, T., and Gassner, G. T. (2005) Mechanism of flavin transfer and oxygen activation by the two-component flavoenzyme styrene monooxygenase, *Arch. Biochem. Biophys.* 442, 102–116.
44. Tu, S.-C., and Hastings, J. W. (1980) Physical interaction and activity coupling between two enzymes induced by immobilization of one, *Proc. Natl. Acad. Sci. U.S.A.* 77, 249–252.
45. Lowry, O. H., Rosebrough, N. J., Farr, A. L., and Randall, R. J. (1951) Protein measurement with the Folin phenol reagent, *J. Biol. Chem.* 193, 265–275.
46. Wang, H., Lei, B., and Tu, S.-C. (2000) *Vibrio harveyi* NADPH-FMN oxidoreductase Arg203 as a critical residue for NADPH recognition and binding, *Biochemistry* 39, 7813–7819.
47. Li, C.-H., and Tu, S.-C. (2005) Active site hydrophobicity is critical to the bioluminescence activity of *Vibrio harveyi* luciferase, *Biochemistry* 44, 12970–12977.
48. Huston, J. S., Levinson, D., Mudgett-Hunter, M., Tai, M. S., Novotny, J., Margolies, M. N., Ridge, R. J., Brucoleri, R. E., Haber, E., Crea, R., and Oppermann, H. (1988) Protein engineering of antibody binding sites: recovery of specific activity in an anti-digoxin single-chain Fv analogue produced in *Escherichia coli*, *Proc. Natl. Acad. Sci. U.S.A.* 85, 5879–5883.
49. Robinson, C. R., and Sauer, R. T. (1998) Optimizing the stability of single-chain proteins by linker length and composition mutagenesis, *Proc. Natl. Acad. Sci. U.S.A.* 95, 5929–5934.
50. Lei, B., Cho, K. W., and Tu, S.-C. (1994) Mechanism of aldehyde inhibition of *Vibrio harveyi* luciferase. Identification of two aldehyde sites and relationship between aldehyde and flavin binding, *J. Biol. Chem.* 269, 5612–5618.
51. Tu, S.-C., and McCormick, D. B. (1974) Conformation of porcine D-amino acid oxidase as studied by protein fluorescence and optical rotatory dispersion, *Biochemistry* 13, 893–899.
52. Liu, M., Lei, B., Ding, Q., Lee, J. C., and Tu, S.-C. (1997) *Vibrio harveyi* NADPH:FMN oxidoreductase: preparation and characterization of the apoenzyme and monomer-dimer equilibrium, *Arch. Biochem. Biophys.* 337, 89–95.
53. Jablonski, E., and DeLuca, M. (1978) Studies of the control of luminescence in *Beneckea harveyi*: properties of the NADH and NADPH:FMN oxidoreductases, *Biochemistry* 17, 672–678.
54. Baldwin, T. O., Nicoli, M. Z., Becvar, J. E., and Hastings, J. W. (1975) Bacterial luciferase. Binding of oxidized flavin mononucleotide, *J. Biol. Chem.* 250, 2763–2768.
55. Duane, W., and Hastings, J. W. (1975) Flavin mononucleotide reductase of luminous bacteria, *Mol. Cell. Biochem.* 6, 53–64.
56. Ballou, D. P., Entsch, B., and Cole, L. J. (2005) Dynamics involved in catalysis by single-component and two-component flavin-dependent aromatic hydroxylases, *Biochem. Biophys. Res. Commun.* 338, 590–598.
57. Brender, J. R., Dertouzos, J., Ballou, D. P., Massey, V., Palfey, B. A., Entsch, B., Steel, D. G., and Gafni, A. (2005) Conformational dynamics of the isoalloxazine in substrate-free *p*-hydroxybenzoate hydroxylase: single-molecule studies, *J. Am. Chem. Soc.* 127, 18171–18178.
58. Tu, S.-C., Romero, F. A., and Wang, L. H. (1981) Uncoupling of the substrate monooxygenation and reduced pyridine nucleotide oxidation activities of salicylate hydroxylase by flavins, *Arch. Biochem. Biophys.* 209, 423–432.
59. Kourtz, L., Dillon, K., Daughtry, S., Madison, L. L., Peoples, O., and Snell, K. D. (2005) A novel thiolase-reductase gene fusion promotes the production of polyhydroxybutyrate in *Arabidopsis*, *Plant Biotechnol. J.* 3, 435–447.
60. Hastings, J. W., and Morin, J. G. (2006) Photons for reporting molecular events: green fluorescent protein and four luciferase systems, *Methods Biochem. Anal.* 47, 15–38.
61. Roda, A., Guardigli, M., Pasini, P., and Mirasoli, M. (2003) Bioluminescence and chemiluminescence in drug screening, *Anal. Bioanal. Chem.* 377, 826–833.

BI701392B